ELSEVIER

Neurobiology of Disease

www.elsevier.com/locate/ynbdi
Neurobiology of Disease 24 (2006) 395–402

Pneumococcal meningitis causes accumulation of neurotoxic kynurenine metabolites in brain regions prone to injury

Caroline L. Bellac, Roney S. Coimbra, Stephan Christen, and Stephen L. Leib*

Institute for Infectious Diseases, University of Bern, Friedbuehlstrasse 51, PO Box 61, CH-3010 Bern, Switzerland

Received 14 June 2006; revised 20 July 2006; accepted 25 July 2006
Available online 7 September 2006

Pneumococcal meningitis (PM) is characterized by an intense inflammatory host reaction that contributes to the development of cortical necrosis and hippocampal apoptosis. Inflammatory conditions in the brain are known to induce tryptophan degradation along the kynurenine pathway, resulting in accumulation of neurotoxic metabolites. In the present study, we investigated the contribution of the kynurenine pathway to brain injury in experimental PM by measuring the concentration of its metabolites and the enzymatic activities and mRNA levels of its major enzymes in the vulnerable brain regions. In the late phase of acute PM, we found a significant transcriptional upregulation of kynurenine-3-hydroxylase and an accumulation of the neurotoxic metabolites 3-hydroxykynurenine (3-HKYN) and 3-hydroxyanthranilic acid in cortex and hippocampus. The positive correlation between the concentration of 3-HKYN and the extent of hippocampal apoptosis adds support to the concept that 3-HKYN contributes to brain injury in PM.

Keywords: Neuroinflammatory diseases; Pneumococcal meningitis; Kynurenine pathway; 3-Hydroxykynurenine; Neurotoxicity; Apoptosis; Brain injury

Introduction

Bacterial meningitis caused by *Streptococcus pneumoniae* is a severe infectious disease of the central nervous system and is associated with acute inflammation and subsequent brain damage. In spite of effective antimicrobial therapy and intensive care, the outcome of pneumococcal meningitis (PM) remains poor with a mortality rate of up to 30% and permanent sequelae due to neuronal injury in up to 50% of the survivors (Schuchat et al., 1997; van de Beek et al., 2004; Weisfelt et al., 2006). Two pathophysiologically different forms of neuronal damage, namely cortical necrosis and hippocampal apoptosis, have been demonstrated in the human disease and corresponding animal models of PM (Bifrare et al., 2003; Nau et al., 1999). Both, the host inflammatory reaction and the pathogen contribute to the brain damage resulting from PM (Grandgirard and Leib, 2006; Koedel et al., 2002).

The pathophysiology of PM is initiated by immune activation that leads to the induction of metabolic pathways in the brain. The kynurenine (KYN) pathway is induced in other diseases associated with inflammation leading to brain injury, such as multiple sclerosis, AIDS-dementia complex and cerebral malaria (Nemeth et al., 2005; Stone, 2001, 2003). Increased tryptophan (TRP) degradation due to activation of the KYN pathway may also be involved in the processes that lead to the neuronal damage observed in PM.

The KYN pathway represents the major catabolic route of the essential amino acid TRP over multiple metabolic steps (Fig. 1). Among the metabolites, some are neurotoxic while others can be neuroprotective. The neurotoxic mechanism of 3-hydroxykynurenine (3-HKYN) and 3-hydroxyanthranilic acid (3-HAA) involves the generation of superoxide and hydrogen peroxide, which contribute to oxidative processes that are implicated in the pathophysiology of PM (Braun et al., 2002; Eastman and Guilarte, 1990). In contrast, kynurenic acid (KYNA) is an antagonist of the excitotoxic *N*-methyl-D-aspartate (NMDA) receptor and protected neurons from excitotoxic brain damage in experimental bacterial meningitis (Leib et al., 1996). The relative concentration of neuroprotective vs. neurotoxic metabolites may thus determine the net effect of the metabolites of the KYN pathway on neuronal damage in PM.

The neurotoxic properties of KYN metabolites and their potential to induce apoptosis (Leavitt et al., 2006; Morita et al., 2001; Okuda et al., 1998) prompted us to assess the role of the KYN pathway in the pathophysiology of PM. With the aim to better understand metabolic changes occurring in vulnerable brain regions during acute PM, we assessed the KYN pathway in cortex (CX) and hippocampus (HC) by three different methods. We quantified KYN metabolites in CX and HC by HPLC and assessed enzymatic activities and mRNA levels of the major enzymes of the KYN pathway in these brain regions. We found the enzyme kynurenine-3-hydroxylase (HK) to be significantly upregulated in the late phase of acute PM. Increased HK activity resulted in accumulation of the neurotoxic metabolites 3-HKYN and 3-HAA in CX and HC. The positive correlation between 3-HKYN concentration and the extent of apoptosis in the HC adds support

* Corresponding author. Fax: +41 31 632 3550.
E-mail address: stephen.leib@ifik.unibe.ch (S.L. Leib).
Available online on ScienceDirect (www.sciencedirect.com).

0969-9961/$ - see front matter © 2006 Elsevier Inc. All rights reserved.
doi:10.1016/j.nbd.2006.07.014

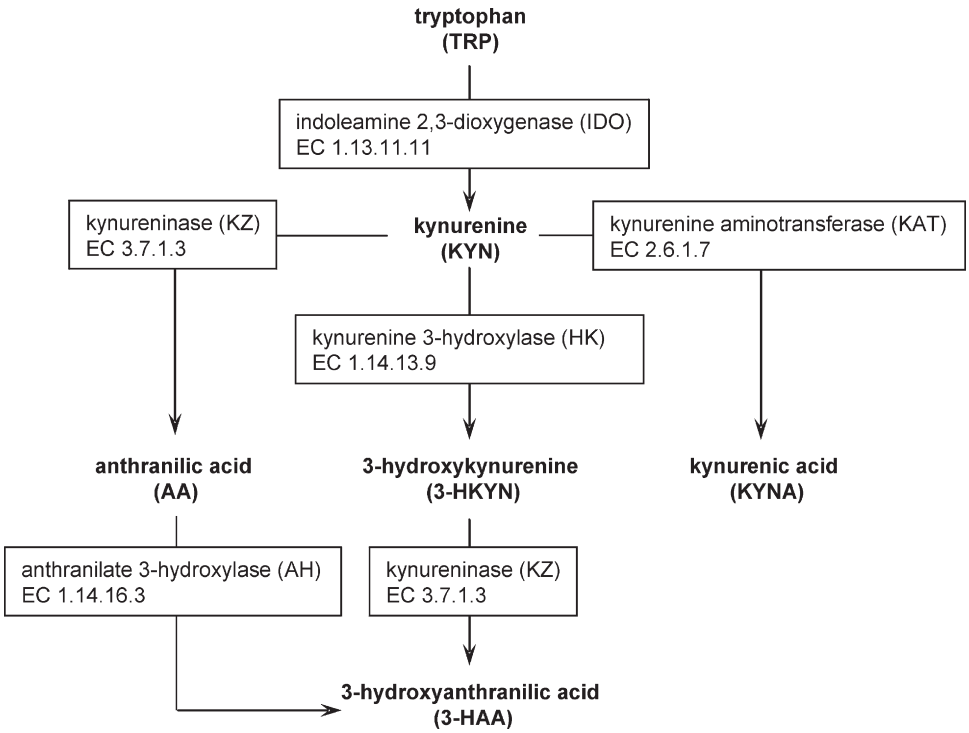

Fig. 1. Simplified schematic of the kynurenine pathway in the rat brain. Tryptophan is metabolized over multiple steps into 3-hydroxyanthranilic acid (3-HAA). Several neuroactive metabolites are included in this pathway: the neuroprotective NMDA-receptor antagonist KYNA and the neurotoxic 3-HKYN and 3-HAA. Conversion of KYN into 3-HKYN is the major route of tryptophan degradation (for the official nomenclature, see KEGG Pathway rno 00380 (Kanehisa)).

to the concept that 3-HKYN contributes to the pathophysiology of brain damage in PM.

Material and methods

Materials

TRP, KYN, 3-HKYN, 3-HAA, KYNA, magnesium chloride hexahydrate, ascorbic acid, D-glucose-6-phosphate, potassium chloride, α-ketoglutaric acid potassium salt, pyridoxal-5-phosphate, β-nicotinamide-adenine-dinucleotide phosphate (NADP), catalase, dATP, dGTP, dTTP and dCTP were obtained from Sigma (St. Louis, MO, USA). Anthranilic acid (AA), zinc acetate dihydrate, TRIS hydrochloride and methylene blue were from Fluka (Buchs, Switzerland). Glucose-6-phosphate-dehydrogenase was from Calbiochem (La Jolla, CA, USA). All other reagents were of HPLC grade and purchased from Merck (Darmstadt, Germany).

Infant rat model of pneumococcal meningitis

The animal studies were approved by the Animal Care and Experimentation Committee of the Canton of Bern, Switzerland, and followed the National Institute of Health's guidelines for the performance of animal experiments.

Wistar rats ($N=86$) were infected intracisternally on postnatal day 11 with 10 µl of saline containing *S. pneumoniae* ($\log_{10}$ 6.4± 0.7 cfu/ml), with a 32-gauge needle (Leib et al., 1998, 2000). Uninfected control animals ($N=23$) were injected with 10 µl of sterile saline solution. Eighteen hours postinfection (p.i.), the animals were clinically assessed (Pfister et al., 2000). Cerebrospinal fluid (CSF) was obtained by puncture of the cisterna magna and 5 µl was cultured qualitatively to document meningitis (Leib et al., 1998). All animals then received antibiotic therapy (Ceftriaxone, 100 mg/kg subcutaneously; Roche Pharma, Reinach, Switzerland). Animals were sacrificed at predetermined time points (i.e. 16 h, 22 h, 36 h or 44 h p.i.) by an overdose of intraperitoneally administered pentobarbital (100 mg/kg). In the animals that were sacrificed at 16 h p.i., the clinical evaluation and the CSF sampling were performed immediately before sacrifice and animals in this group did not receive ceftriaxone.

HPLC measurements of KYN metabolites

Tissue preparation

Infected animals were sacrificed at 16 h ($N=6$), 22 h ($N=8$) and 44 h ($N=8$) p.i., controls at 22 h after mock-infection ($N=6$). After thoracotomy, blood was withdrawn from the right cardiac ventricle with EDTA-treated syringes and processed as described below (determination of TRP metabolites in the plasma). Animals were then perfused with 30 ml ice-cold phosphate buffer saline (PBS) via the left cardiac ventricle. The brains were dissected, rolled on a filter paper to remove the meninges and divided into two hemispheres. From each half of the brain, CX and HC were isolated in ice cold PBS. The CX and HC samples were immediately frozen on dry ice, weighed and stored separately at −80°C until HPLC analysis.

Determination of TRP, KYN, AA, KYNA and 3-HKYN in the brain tissue

Each frozen tissue sample was homogenized in Milli-Q-water (cortex, 1:3 (v/w); hippocampus, 1:5 (v/w)) and acidified with perchloric acid (PCA) 6% (to every 100 µl of the homogenate 25 µl of PCA 6% was added) and centrifuged (10,000×*g*, 4°C,

10 min). The supernatant was filtered (HPLC filter: 0.2 μm; Nylon membrane, Infochroma AG, Zug, Switzerland; 3 ml syringe, Luer, Rodby, Denmark). Eighty microliters of the filtrate was applied onto a C_{18} reverse-phase HPLC column (Supelcosil LC-18-DB, 15 cm × 4.6 mm, 3 μm; Supelco, Buchs, Switzerland) with guard column (Supelguard LC-18-DB, 2 cm). TRP, KYN, AA, KYNA and 3-HKYN were eluted isocratically at a flow rate of 0.8 ml/min with a mobile phase consisting of 100 mM zinc acetate dihydrate and 3% acetonitrile (v/v), pH 6.2 (Wu et al., 2000). TRP and KYN were detected by UV absorption at 280 nm and 360 nm, respectively (L-4250 UV VIS Detector, Merck Hitachi). AA and KYNA were detected by fluorescence (F-1080 Fluorescence Detector, Merck Hitachi) at an excitation of 344 nm and emission of 400 nm. 3-HKYN was detected electrochemically at +0.3 V (Coulochem 5100A, ESA, Chelmsford, MA, USA).

Determination of 3-HAA in the brain tissue

For 3-HAA, 80 μl of CX or HC filtrate was applied onto a C_{18} reverse-phase HPLC column (Supelcosil LC-18-DB, 15 cm × 4.6 mm, 5 μm with 2 cm guard column; Supelco) and eluted isocratically with a mobile phase consisting of 100 mM sodium acetate and 1% acetonitrile, pH 5.0 (Christen and Stocker, 1992) at a flow rate of 1.0 ml/min. 3-HAA was detected electrochemically (Coulochem II, ESA, Chelmsford, MA, USA) at a potential of +0.3 V, after passing the first electrode set at +0.2 V (for removing interfering peaks).

Determination of TRP metabolites in the plasma

The EDTA-treated blood was centrifuged at 7000×*g* at 4°C for 4 min. Plasma was acidified with 25% (v/v) of 6% PCA and frozen on dry ice. At the day of the assay, the sample was centrifuged (10,000×*g*, 4°C, 10 min) and the clear supernatant diluted 1:3 with PCA 1.2%. The diluted plasma was filtered (0.45 μm Nylon membrane, HPLC filter), and 80 μl of the filtrate was analyzed by HPLC as described above.

Enzymatic activity assays

Tissue processing

Infected animals were sacrificed at 22 h (N=10) and 44 h (N=10) p.i., controls at 22 h after mock-infection (N=10). After perfusion with ice-cold PBS, CX and HC were dissected. The frozen tissue was homogenized 1:6 (v/w) in ice-cold homogenization buffer (140 mM potassium chloride/20 mM potassium phosphate, pH 7.0). Homogenates were sonicated, centrifuged at 9000×*g* for 30 min at 4°C and the supernatant collected (Pawlak et al., 2003). Protein concentration in the supernatant was measured with the BCA Protein Assay Kit (Pierce, Rockford, IL, USA). Aliquots of the supernatant were frozen on dry ice and stored at −80°C until analysis. The same homogenate was used for the determination of the enzymatic activities of kynurenine-3-hydroxylase (HK), indoleamine 2,3-dioxygenase (IDO), kynurenine aminotransferase (KAT) and kynureninase (KZ) (see overview in Fig. 1).

The activities of the different enzymes were calculated by subtracting the amount of product present in the reaction mixture at the start of the reaction (i.e. at time point 0 min) from the amount of product present at the investigated time point (e.g. 5 min, 30 min or 60 min). Values were expressed as amount of product formed per minute per mg of protein.

All enzymatic assays were performed with 45 μl of tissue homogenate supernatant and 45 μl of the corresponding substrate solution. Both solutions were separately preincubated for 5 min at 37°C, before they were mixed in a microtiter plate and shaken (200 strokes/min) at 37°C for the assay-specific incubation time. To quantify the amount of product in the reaction mixture, aliquots of 40 μl were taken at 0 min and at the endpoint of incubation time. The samples were acidified with 40 μl of trichloroacetic acid 20% (w/v) and centrifuged at 10,000×*g* for 10 min at 4°C. The supernatant was diluted in mobile phase, frozen on dry ice and stored at −80°C. Eighty microliters of the thawed and filtered mixture was analyzed by HPLC as described above (see HPLC measurements).

Assay of indoleamine 2,3-dioxygenase (IDO) activity

The activity of IDO was quantified by the conversion of TRP to KYN (Saito and Heyes, 1996). The substrate solution consisted of 100 mM potassium phosphate buffer (pH 6.5), 50 μM methylene blue, 200 μg/ml catalase, 50 mM ascorbic acid and 3 mM TRP. Aliquots were taken after 0 and 60 min of incubation. The acidified samples were further incubated for 30 min at 25°C to hydrolyze *N*-formylkynurenine to KYN before centrifugation. The supernatant was diluted 1:2 in mobile phase.

Assay of kynurenine-3-hydroxylase (HK) activity

The activity of HK was measured by the conversion of KYN to 3-HKYN (Saito and Heyes, 1996). The substrate solution consisted of 100 mM potassium phosphate buffer (pH 7.5), 4 mM $MgCl_2$, 3 mM glucose-6-phosphate, 8 U/ml glucose-6-phosphate dehydrogenase, 0.8 mM NADP and 3 mM KYN. Aliquots were taken after 0 min and 5 min of incubation. The supernatant was diluted 1:3 in mobile phase.

Assay of kynurenine aminotransferase (KAT) activity

The activity of KAT was measured by the conversion of KYN to KYNA (Saito and Heyes, 1996). The substrate solution consisted of 200 mM potassium phosphate buffer (pH 8.0), 200 μM pyridoxal phosphate, 20 mM α-ketoglutarate and 3 mM KYN. Aliquots were taken after 0 min and 60 min of incubation. The supernatant was diluted 1:50 in mobile phase.

Assay of kynureninase (KZ) activity

The activity of KZ was measured by the conversion of KYN to AA (Saito and Heyes, 1996). The substrate solution consisted of 200 mM Tris–HCl buffer (pH 8.0), 100 μM pyridoxal phosphate and 3 mM KYN. Aliquots were taken after 0 min and 30 min of incubation. The supernatant was diluted 1:2 in mobile phase.

Analysis of transcriptional expression

RNA isolation

Infected animals were sacrificed at 22 h (N=7) and 44 h (N=7) p.i., controls at 22 h after mock-infection (N=7). The animals were perfused with 30 ml of ice-cold PBS, followed by 30 ml of RNAlater® (Ambion Europe Ltd., Huntingdon, Cambridgeshire, UK) in PBS (v/v 1:2). Whole brains were dissected in ice-cold RNAlater®/PBS (v/v 1:2), and the isolated CX and HC samples were immediately soaked in 200 μl undiluted RNAlater® and stored at 4°C. Total RNA was extracted using the SV Total RNA Isolation System (Promega Corporation, Madison, WI). Sixty milligrams of CX tissue or the whole HC of one hemisphere was homogenized in 1000 μl lysis buffer. Thirty microliters of isolated RNA was further treated with 4 U of RQ1 DNase (Promega). cDNA was made by

reverse transcribing one microgram of total RNA using the enzyme Superscript II (Life Technologies AG, Basel, Switzerland) and random hexameric primers (Promega) according to the manufacturer's instructions.

mRNA quantitation

Transcriptional regulation of the genes *Indo*, *Kmo*, *Kynu* and *Aadat*, encoding the enzymes IDO, HK, KZ and KAT (Fig. 4), respectively, was assessed by comparing their mRNA levels in infected animals at 22 h and 44 h p.i. with those of mock-infected control animals at 22 h p.i. by real-time polymerase chain reaction (PCR) (TaqMan; Applera Europe B.V., Rotkreuz, Switzerland). An ABI PRISM 7000 Sequence Detection System (Applera Europe B.V., Rotkreuz, Switzerland) was used in conjunction with FAM- and NFQ-labeled reporter and quencher paired probes. Primers and probes for all target genes were designed according to the specifications by Applied Biosystems (Assays-by-Design). The sequences to be amplified were chosen across exon/exon boundaries (see Table 1). *Gapdh* was amplified in parallel as control.

cDNA corresponding to 30 ng of reverse transcribed total RNA was amplified in a 25 μl reaction volume using TaqMan Universal PCR Mastermix (Applied Biosystems, Foster City, CA, USA), 22.5 pmol of each primer and 5 pmol of TaqMan probe. Thermal cycling conditions were 2 min at 50°C and 10 min at 95°C for the initial setup, followed by 15 s at 95°C and 1 min at 60°C for each of the 45 cycles. All samples were measured in triplicates. No-template controls and RT-negative controls were included for each RNA sample in each run. For each gene, the mean Δct value of seven control animals was taken to calculate gene expression during infection (at 22 h and 44 h p.i.).

Histopathological examination

Infected animals ($N=30$) were sacrificed at 36 h p.i., when the peak of hippocampal apoptosis occurs in PM (Gianinazzi et al., 2003). The left sided hippocampus was isolated and used for the quantification of 3-HKYN by HPLC, the right half of the brain was fixed in 4% paraformaldehyde in PBS for 12 h, followed by submersion in 18% sucrose for 24 h. Four coronal cryo-sections (45 μm) from the dorsal brain region of each animal were mounted onto polylysine-coated slides and Nissl stained with cresyl violet. Apoptotic damage in the hippocampus was evaluated by histomorphometry as described previously (Bifrare et al., 2003).

Statistics

Data were analyzed by Kruskal–Wallis test (GraphPad Prism, version 4.0, GraphPad Software Inc., San Diego, CA, USA) and differences between groups were tested by Mann–Whitney test. A value of $P<0.05$ was considered statistically significant. Correlation between 3-HKYN and apoptotic score was calculated using Spearman correlation.

Results

Determination of TRP and KYN metabolites in the brain tissue and plasma

Brain levels of 3-HKYN exceeded plasma levels starting at 16 h p.i. and increased continuously for the following hours until 44 h p.i. (Fig. 2). The higher levels in the brain tissue compared to plasma argue for a local production of 3-HKYN within the brain parenchyma. At 44 h p.i., the 3-HKYN concentration in the CX was 10-fold higher than the concentration found in mock-infected animals (590 ± 237 nM vs. 42 ± 15 nM; $P<0.01$). The enzyme KAT alternatively converts 3-HKYN into xanthurenic acid, the brain concentration of which was below the detection limit (i.e. 6 nM) when determined using the same HPLC assay as for the assessment of 3-HAA levels. With the abovementioned exception of 3-HKYN, all other metabolites showed higher concentrations in the plasma than in the brain tissue samples at 16 h, 22 h and 44 h p.i.. Maximal concentrations of TRP, KYN and AA in the brain were measured at 22 h p.i., when the integrity of the blood–brain barrier is compromised by the disease ($P<0.01$ for the concentration of all metabolites in infected animals vs. concentration in mock-infected controls). At 22 h p.i., their brain levels of TRP, KYN and AA were equal or close to plasma levels. Brain concentrations of the neuroprotective KYNA increased only moderately during the observed time period and remained below plasma levels. Except for 3-HAA, all other metabolites showed a similar accumulation kinetic in CX and HC. In contrast, 3-HAA continuously accumulated in the HC over the time period investigated, whereas in CX maximal levels were observed at 22 h p.i. (Fig. 2).

Determination of the enzymatic activities of IDO, HK, KZ and KAT

Accumulation of KYN metabolites was associated with an increase in the enzymatic activities of the upstream enzymes (Figs. 2 and 3). The enzymatic activity of HK and KZ was significantly increased during the acute phase of BM (Fig. 3). HK, which produces the neurotoxic 3-HKYN, was 2.4-fold more active in the CX at 22 h p.i. and 3-fold more at 44 h p.i. compared to the activity found in mock-infected animals ($P<0.05$). In the HC, HK activity reached a plateau at 22 h p.i. For KZ, the highest enzymatic activity was found at 22 h p.i. (2-fold higher compared to control animals ($P<0.05$)). The enzyme KAT showed decreased activity during the disease ($P<0.01$ at 44 h p.i.) compared to the activity found in mock-infected animals (Fig. 3).

Table 1
Primers used for the analysis of transcriptional expression

Rat gene	Gene ID	Forward primer	Reverse primer	Probe
Indo	66029	CTTCGTGGATCCAGACACCTTTT	CCCTCCGGCAGCTTAGG	CCCTTCCAACCAGACAAA
Kmo	59113	GGAGCTGACAATTCCACCTAAGAAC	TTTCTAGGCCAAATGTGAAGACAGTT	CCATGGCATACTCCCC
Kynu	116682	CCAAAGCGGCACAAAATTCTTCTAG	CCATGAAGTTGAATCTGTGACTCGAT	TTCCCTTCTGATCATTATGC
Aadat	29416	CCCTGTGTTCGTGACTCTGAAG	GATCCAGTTGCCAATCATTGCT	CCGAGCCCTGCTCCT
Gapdh [a]	24383			AAACCCATCACCATCTTCCAGGAGC

[a] Primer pre-designed by Applied Biosystems (Assays-on-Demand).

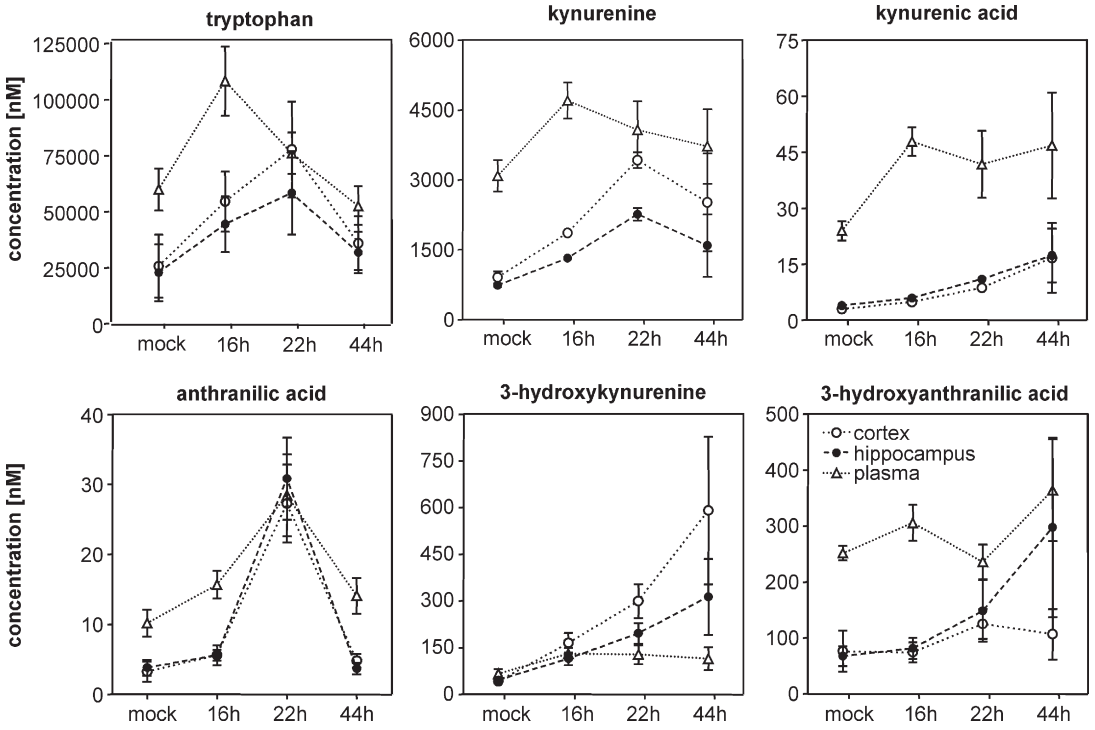

Fig. 2. Concentrations of different TRP metabolites during acute PM, measured at 16 h, 22 h and 44 h p.i. and at 22 h in mock-infected controls in CX, HC and plasma. The neurotoxic metabolite 3-hydroxykynurenine (3-HKYN) is markedly increased in CX and HC of infected animals over the entire disease progression, while in plasma no increase is observed. All other metabolites showed higher concentrations in the plasma than in the brain. Values are mean±SEM. Significant differences between infected and mock-infected animals in the brain were detected at 22 h p.i. ($P<0.01$) for all the metabolites and at 44 h p.i. for 3-HKYN ($P<0.01$).

We measured low enzymatic activity for the enzyme IDO in the brain of mock-infected control animals as well as during acute PM (Fig. 3). As a control for the enzymatic assay, we determined IDO activity in the lung and spleen of mock-infected animals. Consistent with the literature (Fujigaki et al., 1998; Heyes et al., 1997), we found higher basal IDO activity in the lung (1.4 pmol KYN/min/mg protein, $N=5$) and spleen (0.7 pmol KYN/min/mg protein, $N=5$) than in the brain (0.4 pmol KYN/min/mg protein in CX, $N=10$, <0.2 pmol KYN/min/mg protein in HC, $N=5$).

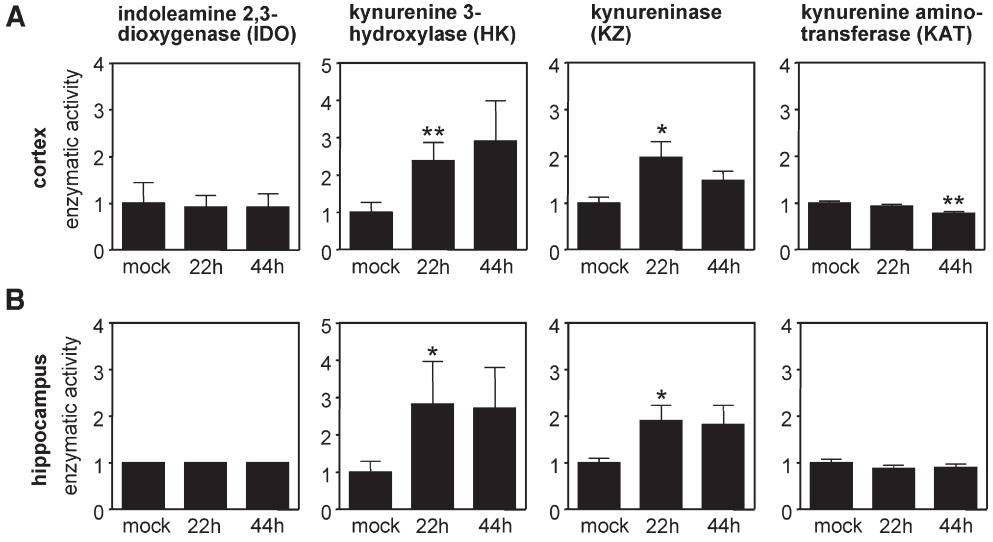

Fig. 3. Enzymatic activities of the major enzymes of the KYN pathway during acute PM, determined in infected animals (at 22 h and 44 h p.i.) and in mock-infected controls (at 22 h p.i.) in CX (A) and HC (B). Enzymatic activities are expressed as fold increase of activity in mock-infected animals. Increased enzymatic activity was found for HK and KZ at 22 h p.i. Values are mean±SD. Differences between mock-infected and infected animals are indicated as *$P<0.05$; **$P<0.01$. (A) $N=10$ in each group, (B) $N=5$ in each group, except for HK $N=10$.

Transcriptional expression of IDO, HK, KZ and KAT

Transcriptional regulation of the genes *Indo*, *Kmo*, *Kynu*, and *Aadat*, encoding the enzymes IDO, HK, KZ and KAT, respectively, was determined by comparing their mRNA levels in the CX and HC of infected animals at 22 h and 44 h p.i with mRNA levels in the CX and HC from mock-infected controls at 22 h (Fig. 4). We found increased *Kmo* mRNA levels at the late phase of acute PM (i.e. at 44 h p.i.). At 44 h p.i., mRNA levels of *Kmo* were 4.4-fold higher in the CX ($P<0.01$) and 6.1-fold higher in the HC ($P<0.05$) than in mock-infected animals. Beside *Kmo*, we only detected increased mRNA levels for *Kynu* at 44 h p.i. in the HC (2.6-fold higher, $P<0.01$). No other gene investigated was differentially regulated as a consequence of PM during the time points assessed in this study.

Correlation between 3-HKYN concentration and neuronal injury in the hippocampus

Only infected animals were included in the evaluation. 3-HKYN concentration in the HC assessed at 36 h p.i. positively correlated with the extent of hippocampal apoptotic damage assessed in the same animals at 36 h p.i. ($P<0.01$; Spearman $r=0.5$) (see Fig. 5). All animals with apoptotic score >0.5 showed high 3-HKYN concentrations (200 nM–1300 nM) in the HC.

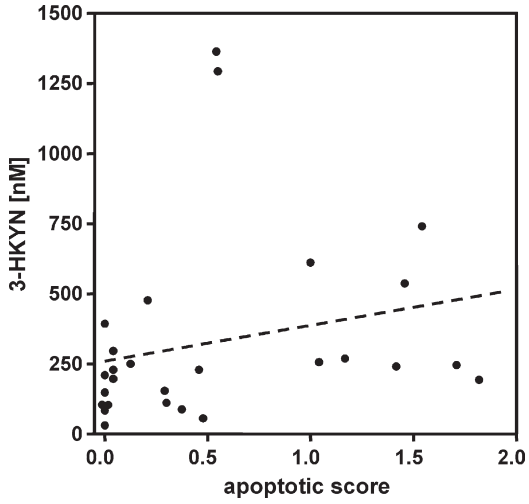

Fig. 5. Correlation between 3-HKYN concentration and apoptotic damage in the hippocampus at 36 h p.i.. Only infected animals ($N=30$) were included in the calculation of the correlation. The mean value of 4 evaluated cryoslides per animal was used to calculate apoptotic damage. Apoptotic score 0: 0–5 apoptotic cells; score 1: 6–20 apoptotic cells; score 2: over 20 apoptotic cells. All animals with apoptotic score >0.5 showed 3-HKYN concentrations >190 nM. Significant correlation between 3-HKYN and apoptosis was found (Spearman correlation $P<0.01$, $r=0.5$).

Discussion

The KYN pathway has been shown to play an important role in the pathophysiology of neuroinflammatory diseases (Nemeth et al., 2005; Stone, 2001; Stone et al., 2003). In the present study, we demonstrate that the host response to PM leads to accumulation of neurotoxic KYN metabolites in the brain. We measured increased concentrations of 3-HKYN and 3-HAA in the late phase of acute PM i.e. at 44 h p.i. The positive correlation between the concentration of 3-HKYN and the extent of apoptotic damage in the HC suggests a role for 3-HKYN in the pathophysiology of brain injury in PM.

The temporal changes in the levels of the different KYN metabolites offer some insight as to the mechanisms of how they accumulate in the CX and HC during PM. 3-HKYN showed a different kinetic of accumulation in the brain in comparison with the two metabolites AA and KYNA that are formed from the same precursor KYN (Fig. 1). Whereas brain AA concentrations peaked at 22 h p.i., when the integrity of the blood–brain barrier is compromised by the disease (Meli et al., 2006; Schaper et al., 2003), the concentrations of 3-HKYN continuously increased from 16 h to 44 h in the CX and HC (Fig. 2). The comparison of the levels of 3-HKYN in plasma (115 nM) with those in CX (590 nM) and HC (313 nM) at 44h p.i. argues for an augmented local production within the brain parenchyma as the cause for the increase in 3-HKYN in the brain. In line with this concept, the increase of 3-HKYN concentrations was

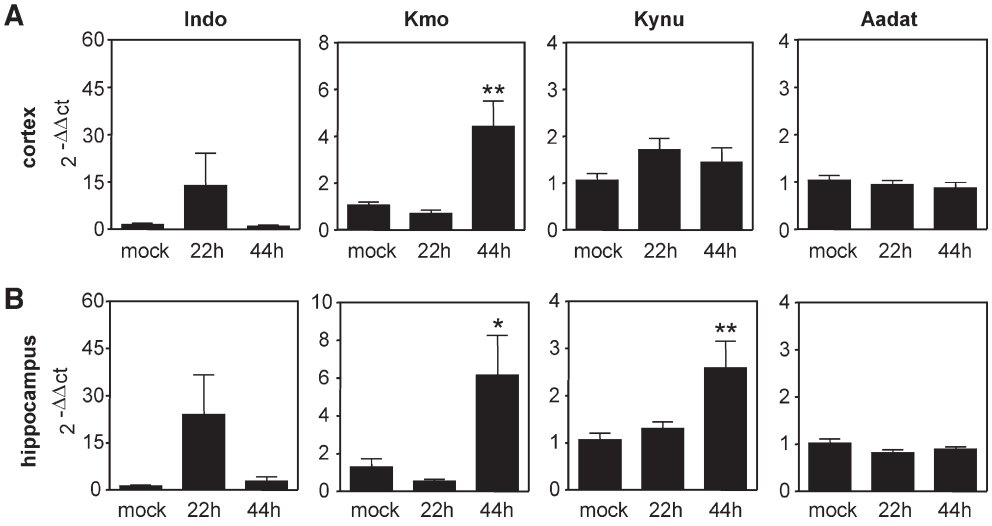

Fig. 4. mRNA levels of the genes *Indo*, *Kmo*, *Kynu* and *Aadat* encoding the enzymes IDO, HK, KZ and KAT, respectively, quantified by real-time PCR at 22 h ($N=7$) and 44 h ($N=7$) p.i. and at 22 h in mock-infected controls ($N=7$) in CX (A) and HC (B). Amplification of endogenous *Gapdh* was used for normalization of transcriptional expression. mRNA levels of infected animals are indicated relatively to those of mock-infected animals. Differences between mock-infected and infected animals are marked as $*P<0.05$; $**P<0.01$.

associated with increased *Kmo* mRNA levels at 44 h p.i. and increased HK activity in CX and HC at 22 h and 44 h p.i. (Figs. 3 and 4). These findings are in agreement with previous findings in the model from microarray studies, showing *Kmo* upregulation in CX and HC of infected animals with acute PM (Coimbra et al., 2006).

The rate-limiting step in KYN formation is the induction of IDO. However, we did not find increased IDO activity during PM in brain parenchyma. This lack of increase in IDO activity contrasts with data from other studies in models of neuroinflammation that found accumulation of neurotoxic KYN metabolites as a result of IDO induction (Adam et al., 2005; Brown et al., 1991). Basal activity of IDO in control brains was at or below the detection limit of the assay used in the present study (0.2 pmol/min/mg protein) and the activity remained low in PM (Fig. 3). Even though we measured increased levels of *Indo* mRNA at the early acute phase of the disease (22 h p.i.), the enzymatic activity of IDO remained low (Figs. 3 and 4). The activity of IDO may be attenuated by counter regulatory factors in PM. One of which could be nitric oxide (NO), which has shown to be highly increased during the acute phase of PM as a result of inducible nitric oxide synthase (iNOS) induction (Hucke et al., 2004; Leib et al., 1998; Winkler et al., 2001). Nonetheless, we detected increased brain levels of the product of IDO, namely KYN, at 22 h and 44 h p.i. The kinetic of changes in the concentrations of KYN in plasma and brain is similar to that of its precursor TRP (Fig. 2). The concentrations of both metabolites are higher in the plasma than in the brain. Whereas the concentrations of KYN and TRP in plasma peak at 16 h p.i., the maximum concentrations in the brain are found at 22 h p.i., when the blood–brain barrier (BBB) is partially disrupted by the disease (Meli et al., 2006; Schaper et al., 2003). Leakage of the metabolites from the plasma into the brain may contribute to their increase in CX and HC. The increased enzymatic activity of HK coupled with a facilitated diffusion of KYN trough the leaky BBB likely leads to the observed increase of 3-HKYN levels in CX and HC.

Concentrations of 3-HKYN measured in the CX at 44 h p.i. (600 nM) are close to those previously shown to be neurotoxic in cell cultures (1000 nM) (Okuda et al., 1996). The known neurotoxic features of 3-HKYN, such as apoptosis and increase in ROS concentration, are consistent with the observed histopathological manifestations of PM (Bifrare et al., 2003; Jeong et al., 2004; Okuda et al., 1996; Okuda et al., 1998). In addition to the increased 3-HKYN levels, we also found 3-HAA to accumulate in CX and HC during acute PM (Fig. 2). However, differently from 3-HKYN, 3-HAA accumulates only in the HC, and only in the later phase of acute PM (44 h p.i.). This process involves the transcriptional upregulation of *Kynu* specifically in the HC. 3-HAA was also shown to induce apoptosis (Morita et al., 2001). Furthermore, increased 3-HAA concentrations can result in elevated QUINA levels, a downstream metabolite in the KYN pathway, which is also a potent neurotoxin implicated in neuroinflammatory diseases (Guillemin et al., 2005).

KYNA, a potential neuroprotectant, was only moderately increased in the brain (Fig. 2). Interestingly, we found lower *Aadat* mRNA levels and lower enzymatic activity of the corresponding enzyme KAT in infected compared to mock-infected animals (Figs. 3 and 4). A KYNA concentration of 30–60 μM is a prerequisite for a neuroprotective effect of KYNA by antagonism on the NMDA receptor (Obrenovitch and Urenjak, 2000; Urenjak and Obrenovitch, 2000). However, this concentration is two magnitudes above the KYNA levels measured in the present study. Thus, the balance of the relative concentration of potential neuroprotective vs. neurotoxic metabolites in infected animals is dominated by potential neurotoxic metabolites.

In summary, the present study demonstrated that the host response to PM in infant rats involves an increased production of the neurotoxic metabolites 3-HKYN and 3-HAA in CX and HC during the acute disease. The increase in 3-HKYN concentrations in the brain corresponds to increased transcription and increased enzymatic activity of the enzyme HK during acute PM. The positive correlation found between 3-HKYN concentrations and the extent of apoptotic damage in the HC suggests that increased production of 3-HKYN may play a role in the pathophysiologic processes leading to neuronal injury in PM.

Acknowledgments

We thank Angela Bühlmann and Jürg Kummer for excellent technical support.

This work was supported by grants from the Swiss National Science Foundation (grants 632-066057, 32-066845, 31-108236), by the NIH (2P50NS035902-06 and R01NS33997) and by the Roche Research Foundation (grant mkl/stm 55-2005).

References

Adam, R., Russing, D., Adams, O., Ailyati, A., Sik Kim, K., Schroten, H., Daubener, W., 2005. Role of human brain microvascular endothelial cells during central nervous system infection. Significance of indoleamine 2,3-dioxygenase in antimicrobial defence and immunoregulation. Thromb. Haemostasis 94, 341–346.

Bifrare, Y.D., Gianinazzi, C., Imboden, H., Leib, S.L., Täuber, M.G., 2003. Bacterial meningitis causes two distinct forms of cellular damage in the hippocampal dentate gyrus in infant rats. Hippocampus 13, 481–488.

Braun, J.S., Sublett, J.E., Freyer, D., Mitchell, T.J., Cleveland, J.L., Tuomanen, E.I., Weber, J.R., 2002. Pneumococcal pneumolysin and H (2)O(2) mediate brain cell apoptosis during meningitis. J. Clin. Invest. 109, 19–27.

Brown, R.R., Ozaki, Y., Datta, S.P., Borden, E.C., Sondel, P.M., Malone, D.G., 1991. Implications of interferon-induced tryptophan catabolism in cancer, auto-immune diseases and AIDS. Adv. Exp. Med. Biol. 294, 425–435.

Christen, S., Stocker, R., 1992. Simultaneous determination of 3-hydroxyanthranilic and cinnabarinic acid by high-performance liquid chromatography with photometric or electrochemical detection. Anal. Biochem. 200, 273–279.

Coimbra, R.S., Voisin, V., de Saizieu, A.B., Lindberg, R.L., Leppert, D., Wittwer, M., Leib, S.L., 2006. Gene expression in cortex and hippocampus during acute pneumococcal meningitis. BMC Biol. 4, 15.

Eastman, C.L., Guilarte, T.R., 1990. The role of hydrogen peroxide in the in vitro cytotoxicity of 3-hydroxykynurenine. Neurochem. Res. 15, 1101–1107.

Fujigaki, S., Saito, K., Takemura, M., Fujii, H., Wada, H., Noma, A., Seishima, M., 1998. Species differences in L-tryptophan-kynurenine pathway metabolism: quantification of anthranilic acid and its related enzymes. Arch. Biochem. Biophys. 358, 329–335.

Gianinazzi, C., Grandgirard, D., Imboden, H., Egger, L., Meli, D., Bifrare, Y.-D., Joss, P., Täuber, M., Borner, C., Leib, S., 2003. Caspase-3 mediates hippocampal apoptosis in pneumococcal meningitis. Acta Neuropathol. (Berl.) 105, 499–507.

Grandgirard, D., Leib, S.L., 2006. Strategies to prevent neuronal damage in paediatric bacterial meningitis. Curr. Opin. Pediatr. 18, 112–118.

Guillemin, G.J., Wang, L., Brew, B.J., 2005. Quinolinic acid selectively induces apoptosis of human astrocytes: potential role in AIDS dementia complex. J. Neuroinflammation. 2, 16.

Heyes, M.P., Saito, K., Chen, C.Y., Proescholdt, M.G., Nowak, T.S., Li, J., Beagles, K.E., Proescholdt, M.A., Zito, M.A., Kawai, K., Markey, S.P., 1997. Species heterogeneity between gerbils and rats: quinolinate production by microglia and astrocytes and accumulations in response to ischemic brain injury and systemic immune activation. J. Neurochem. 69, 1519–1529.

Hucke, C., MacKenzie, C.R., Adjogble, K.D., Takikawa, O., Daubener, W., 2004. Nitric oxide-mediated regulation of gamma interferon-induced bacteriostasis: inhibition and degradation of human indoleamine 2,3-dioxygenase. Infect. Immun. 72, 2723–2730.

Jeong, J.H., Kim, H.J., Lee, T.J., Kim, M.K., Park, E.S., Choi, B.S., 2004. Epigallocatechin 3-gallate attenuates neuronal damage induced by 3-hydroxykynurenine. Toxicology 195, 53–60.

Kanehisa, L., KEGG: Kyoto Encyclopedia of Genes and Genomes http://www.genome.jp/dbget-bin/get_pathway?org_name=rno& mapno=00380.

Koedel, U., Scheld, W.M., Pfister, H.W., 2002. Pathogenesis and pathophysiology of pneumococcal meningitis. Lancet, Infect Dis. 2, 721–736.

Leavitt, B.R., Raamsdonk, J.M., Shehadeh, J., Fernandes, H., Murphy, Z., Graham, R.K., Wellington, C.L., Raymond, L.A., Hayden, M.R., 2006. Wild-type huntingtin protects neurons from excitotoxicity. J. Neurochem. 96, 1121–1129.

Leib, S.L., Kim, Y.S., Ferriero, D.M., Täuber, M.G., 1996. Neuroprotective effect of excitatory amino acid antagonist kynurenic acid in experimental bacterial meningitis. J. Infect. Dis. 173, 166–171.

Leib, S.L., Kim, Y.S., Black, S.M., Tureen, J.H., Täuber, M.G., 1998. Inducible nitric oxide synthase and the effect of aminoguanidine in experimental neonatal meningitis. J. Infect. Dis. 177, 692–700.

Leib, S.L., Leppert, D., Clements, J., Täuber, M.G., 2000. Matrix metalloproteinases contribute to brain damage in experimental pneumococcal meningitis. Infect. Immun. 68, 615–620.

Meli, D.N., Coimbra, R.S., Erhart, D.G., Loquet, G., Bellac, C.L., Täuber, M.G., Neumann, U., Leib, S.L., 2006. Doxycycline reduces mortality and injury to the brain and cochlea in experimental pneumococcal meningitis. Infect. Immun. 74, 3890–3896.

Morita, T., Saito, K., Takemura, M., Maekawa, N., Fujigaki, S., Fujii, H., Wada, H., Takeuchi, S., Noma, A., Seishima, M., 2001. 3-Hydroxyanthranilic acid, an L-tryptophan metabolite, induces apoptosis in monocyte-derived cells stimulated by interferon-gamma. Ann. Clin. Biochem. 38, 242–251.

Nau, R., Soto, A., Bruck, W., 1999. Apoptosis of neurons in the dentate gyrus in humans suffering from bacterial meningitis. J. Neuropathol. Exp. Neurol. 58, 265–274.

Nemeth, H., Toldi, J., Vecsei, L., 2005. Role of kynurenines in the central and peripheral nervous systems. Curr. Neurovasc. Res. 2, 249–260.

Obrenovitch, T.P., Urenjak, J., 2000. In vivo assessment of kynurenate neuroprotective potency and quinolinate excitotoxicity. Amino Acids 19, 299–309.

Okuda, S., Nishiyama, N., Saito, H., Katsuki, H., 1996. Hydrogen peroxide-mediated neuronal cell death induced by an endogenous neurotoxin, 3-hydroxykynurenine. Proc. Natl. Acad Sci. U. S. A. 93, 12553–12558.

Okuda, S., Nishiyama, N., Saito, H., Katsuki, H., 1998. 3-Hydroxykynurenine, an endogenous oxidative stress generator, causes neuronal cell death with apoptotic features and region selectivity. J. Neurochem. 70, 299–307.

Pawlak, D., Tankiewicz, A., Matys, T., Buczko, W., 2003. Peripheral distribution of kynurenine metabolites and activity of kynurenine pathway enzymes in renal failure. J. Physiol. Pharmacol. 54, 175–189.

Pfister, L.A., Tureen, J.H., Shaw, S., Christen, S., Ferriero, D.M., Täuber, M. G., Leib, S.L., 2000. Endothelin inhibition improves cerebral blood flow and is neuroprotective in pneumococcal meningitis. Ann. Neurol. 47, 329–335.

Saito, K., Heyes, M.P., 1996. Kynurenine pathway enzymes in brain. Properties of enzymes and regulation of quinolinic acid synthesis. Adv. Exp. Med. Biol. 398, 485–492.

Schaper, M., Leib, S.L., Meli, D.N., Brandes, R.P., Täuber, M.G., Christen, S., 2003. Differential effect of p47phox and gp91phox deficiency on the course of pneumococcal meningitis. Infect. Immun. 71, 4087–4092.

Schuchat, A., Robinson, K., Wenger, J.D., Harrison, L.H., Farley, M., Reingold, A.L., Lefkowitz, L., Perkins, B.A., 1995. Bacterial meningitis in the United States in 1995. Active Surveillance Team. N. Engl. J. Med. 337, 970–976.

Stone, T.W., 2001. Kynurenines in the CNS: from endogenous obscurity to therapeutic importance. Prog. Neurobiol. 64, 185–218.

Stone, T.W., Mackay, G.M., Forrest, C.M., Clark, C.J., Darlington, L.G., 2003. Tryptophan metabolites and brain disorders. Clin. Chem. Lab. Med. 41, 852–859.

Urenjak, J., Obrenovitch, T.P., 2000. Neuroprotective potency of kynurenic acid against excitotoxicity. NeuroReport 11, 1341–1344.

van de Beek, D., de Gans, J., Spanjaard, L., Weisfelt, M., Reitsma, J.B., Vermeulen, M., 2004. Clinical features and prognostic factors in adults with bacterial meningitis. N. Engl. J. Med. 351, 1849–1859.

Weisfelt, M., van de Beek, D., Spanjaard, L., Reitsma, J.B., de Gans, J., 2006. Clinical features, complications, and outcome in adults with pneumococcal meningitis: a prospective case series. Lancet Neurol. 5, 123–129.

Winkler, F., Koedel, U., Kastenbauer, S., Pfister, H.W., 2001. Differential expression of nitric oxide synthases in bacterial meningitis: role of the inducible isoform for blood–brain barrier breakdown. J. Infect. Dis. 183, 1749–1759.

Wu, H.Q., Guidetti, P., Goodman, J.H., Varasi, M., Ceresoli-Borroni, G., Speciale, C., Scharfman, H.E., Schwarcz, R., 2000. Kynurenergic manipulations influence excitatory synaptic function and excitotoxic vulnerability in the rat hippocampus in vivo. Neuroscience 97, 243–251.